Mathematical Modelling of the Influence of Different Concentrations of Oxaloacetate to Glycerol-3-Phosphate Dehydrogenase Structure

Nataliya A. Kolotyeva[1*], Frida N. Gilmiyarova[1], Oksana A. Gusyakova[1], Marina V. Komarova[2], Nikita V. Remizov[2], and Elena A. Ryskina[3]

[1] Samara State Medical University, 89 Chapaevskaya str, Samara 443099, Russia
[2] Samara National Research University, 34 Moskovskoe shosse, Samara 443086, Russia
[3] Higher School of Economics, 20 Myasnitskaya str., Moscow 101000, Russia

*** e-mail:** n.a.koloteva@samsmu.ru

Abstract. The study was devoted to the influence of different concentrations of oxaloacetate on the conformational structure of glycerol-3-phosphate dehydrogenase in a temperature gradient, using differential scanning fluorimetry on a Prometheus NT.48 device (NanoTemper Technologies, Germany). We studied the fluorescence ratio (350/330 nm) of glycerol-3-phosphate dehydrogenase in the presence of oxaloacetate at concentrations of 0.5–16 μM in a temperature gradient of 20–95 °C. We built linear regression models for the physiological temperature range and nonlinear models (polynomial of the third degree) for the temperature range corresponding to protein melting. Temperature was the independent variable; fluorescence ratio was the variable. The effect of different oxaloacetate concentrations on glycerol-3-phosphate dehydrogenase thermostability was evaluated by comparing the parameters of obtained regression models. At the physiological temperature range of 20–40 °C, the fluorescence ratios and their growth rates at oxaloacetate concentrations of 0.5-8 μM ($p < 0.001$) were found to be lower than those of controls. Higher average fluorescence ratios and growth rates were detected at oxaloacetate concentrations of 16 μM ($p < 0.001$). When heating over 45 °C, no differences were found in the average denaturation temperature of glycerol-3-phosphate dehydrogenase between the oxaloacetate concentrations studied. The experiment demonstrates the change in the total amplitude of the fluorescence signal in the process of heating the enzyme. The effect of biologically active compounds on fluorescence ratio differs in the area of low concentrations (0.5 and 1 μM) and high concentrations (16 μM). Oxaloacetate at a final concentration of 0.5–1 μM contributes to the thermodynamic stability of glycerol-3-phosphate dehydrogenase, while the concentration of 16 μM causes a decrease in its thermostability.

Keywords: glycerol-3-phosphate dehydrogenase; oxaloacetate; differential scanning fluorimetry; conformation structure; mathematical modelling.

Paper #3462 received 02 Nov 2021; accepted for publication 28 Feb 2022; published online 21 Mar 2022. doi: 10.18287/JBPE22.08.010302.

1 Introduction

In recent years, there has been an increasing interest in small molecules – compounds with a molecular mass between 40 and 1000 Da – that can change the content of metabolites and their fluxes in the pathways of intermediate metabolism, which can regulate specific intermolecular processes. The study of small molecules today seems to be an urgent task because, having a very

small molecular weight, they have multiple effects not only on metabolism in general, but also on intercellular interaction systems [1–4].

Glycerol-3-phosphate dehydrogenase (EC 1.1.1.8, GPDH), is a NAD-dependent dehydrogenase located at the crossroads of the metabolic pathways of carbohydrate and fat metabolism, whose structural and functional potential enables numerous biomolecular processes. Dihydroxyacetone phosphate and the redox partner, glycerol 3-phosphate, are substrates of the reaction. With a lack of energy, the dihydroxyacetone phosphate molecule continues its way in the glycolytic process; if there is enough energy, it can enter the lipid biosynthesis pathway [5, 6]. Numerous metabolic and non-metabolic functions of these switches are provided by gentle regulation by GPDH. Mitochondrial GPDH has been shown to accelerate glucose oxidation by stimulating acetyl coenzyme A production, histone acetylation, and induction of genes encoding inflammatory mediators in macrophages, promoting oncogenesis in glioma cells [7, 8]. The study of GPDH represents a therapeutic target for treatment and mechanisms of cancer regulation [9–11].

Oxaloacetate (OA) is a metabolic intermediate, a valuable and rather rare molecule, its concentration in mitochondria does not exceed 10^{-6} M [12], participates in many metabolic pathways, including gluconeogenesis, the citric acid cycle, the glyoxylate cycle, amino acid synthesis, fatty acid synthesis. Oxaloacetate is a critical component in ATP production and must be continuously regenerated for the citric acid cycle and electron transfer chain to continue. Oxaloacetate is important not only as a molecular switch and mediator in complex biological processes. Due to its central role in energy metabolism, it has been called a bioenergetic drug specifically designed to increase cellular energy levels, has protective, promitochondrial actions, prevents neuroinflammation, neurodegeneration [13–15].

The use of the differential scanning fluorimetry method makes it possible to evaluate protein folding as well as its conformational and colloidal stability under various thermal and chemical conditions. The principle of the method is based on changes in the endogenous fluorescence of tryptophan and tyrosine, which is very sensitive and changes with thermal unfolding. Using a thermal gradient causes denaturation of the tertiary structure, the protein unfolds, which contributes to the escape of hydrophobic sites with tryptophan from the pockets. This leads to a shift in the fluorescence peaks; differential scanning fluorimetry tracks these changes with high temporal resolution and can even detect several unfolding transitions [16].

This study focuses on the effect of different concentrations of oxaloacetate on the conformational structure of glycerol-3-phosphate dehydrogenase in a temperature gradient, followed by the study of fluorescence curves and fitting mathematical model.

2 Materials and Methods

2.1 The Experiment overview

The experiments were performed in the Laboratory of Molecular and Radiation Biophysics at the National Research Center “Kurchatov Institute”.

We used reagents from Sigma-Aldrich, USA: catalytic protein glycerol-3-phosphate dehydrogenase, oxaloacetate, 50 mM Tris-HCl buffer, pH 7.5. The pH value was monitored before and after adding the small molecule solution to the samples using a Mettler Toledo pH-meter (USA). The change in pH of the medium had fluctuations within the range of 0.01–0.02.

The conformational structure of glycerol-3-phosphate dehydrogenase protein molecules under the influence of oxaloacetate was determined using Differential Scanning Fluorimetry (DSF) on a Prometheus NT.48 instrument (NanoTemper Technologies, Germany). The conformational stability of the protein was described by its average denaturation temperature Tm (°C), which is the point where half of the protein unfolds. The principle of differential scanning fluorimetry is based on the change in endogenous fluorescence of tryptophan and tyrosine at 330 and 350 nm, which changes with thermal unfolding [17]. Six dilutions were prepared in which the final concentration of GPDH was constant, 1 μM, and the final concentration of oxaloacetate solution varied: 0.5 μM, 1 μM, 2 μM, 4 μM, 8 μM, and 16 μM. We placed 10 μl of the prepared solution into Prometheus NT.48, nanoDSF grade capillaries (Germany). Scanning fluorimetry was performed at a laser intensity of 30%, heating range from 20 °C to 95 °C, step 1 °C/min.

2.2 Statistical Analyses

Mathematical modeling of fluorescence ratio curves as a function of temperature and oxaloacetate concentration and statistical analysis of obtained parameters of regression equations were performed using SPSS v. 25 (IBM Corporation, Armonk, New York, USA). We used linear models and analysis of covariance (ANCOVA) for the physiological temperature range, approximation by cubic regression to investigate protein melting point. To assess the quality of fitted models, we examined regression residuals, calculated coefficients of determination (R^2) and standard errors of regression (SE regr). A two-tailed p-value < 0.05 was considered statistically significant.

3 Results and Discussion

Preliminary visual analysis of the melting curves of GPDH without ligand and with the oxaloacetate (Fig. 1) makes it possible to distinguish several sites that differ in biochemical nature. In the physiological temperature range (up to 45–50 °C) there is a linear increase in the fluorescence ratio, at a temperature of the order of 50–55°C – melting, and at higher temperatures – a subsequent increase in the fluorescence ratio.

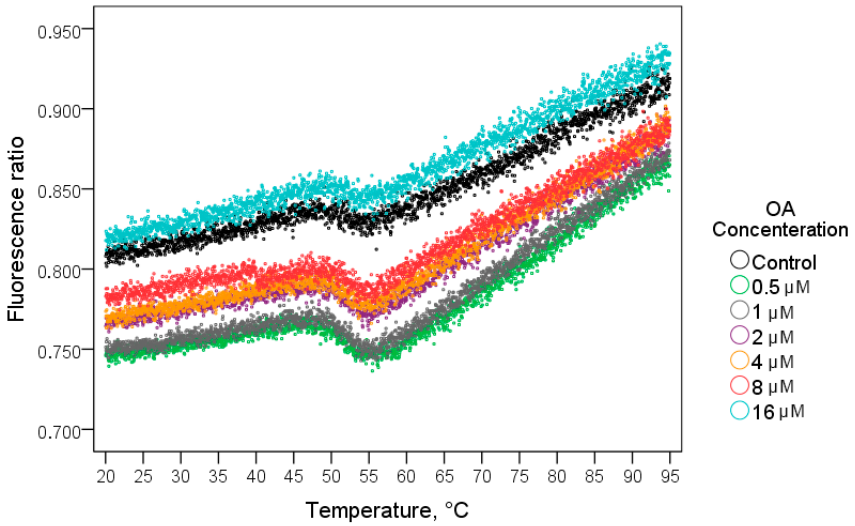

Fig. 1 Ratio of fluorescences at different concentrations of oxaloacetate during GPDH heating in the temperature range 20–95 °C.

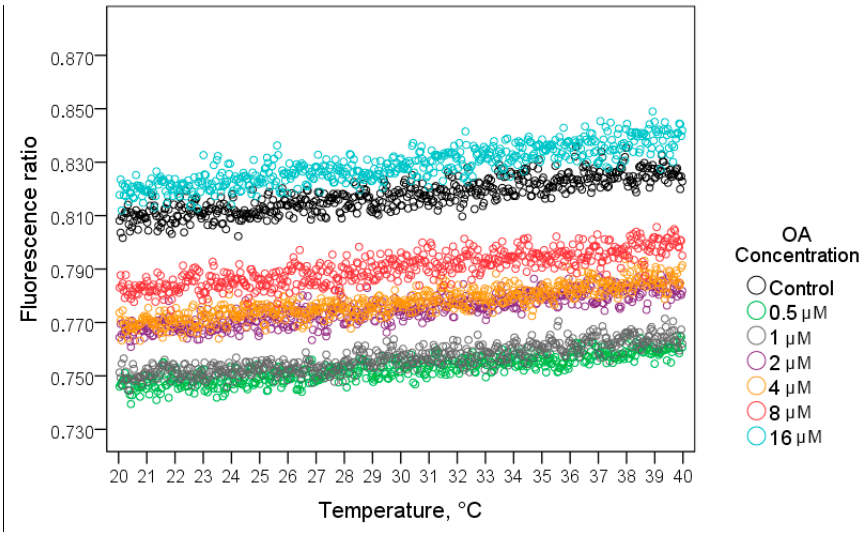

Fig. 2 Ratio of fluorescences at different concentrations of oxaloacetate during GPDH heating in the temperature range 20–40 °C.

Table 1 Summary of linear models of the relationship of GPDH fluorescence to temperature in the range from 20 to 40 °C when oxaloacetate is added at different concentrations.

Concentration of oxaloacetate	**Intercept, × 10^{-3}**		**Slope, × 10^{-3}**		**Model Quality Assessment**	
	b_0	SE b_0	b_1	SE b_1	R^2	SE regr
Control	789.1	0.77	0.95	0.025	0.72	3.43
0.5 µM	731.5	0.58	0.71	0.019	0.70	2.59
1 µM	733.6	0.62	0.77	0.020	0.73	2.77
2 µM	749.8	0.66	0.84	0.022	0.74	2.91
4 µM	751.3	0.68	0.88	0.022	0.77	2.99
8 µM	764.1	0.77	0.88	0.025	0.76	3.42
16 µM	797.5	0.83	1.05	0.027	0.70	3.68

Note: b_0 – constant; SE b_0 – standard errors of constant; b_1 – regression coefficients; SE b_1 – standard errors of regression coefficients; R^2 – coefficient of determination; SE regr – standard errors of regression.

At the first stage, we isolated the temperature range corresponding to the physiological norm from 20 to 40 °C (Fig. 2) and compared the average values of the fluorescence ratio in the presence of different concentrations of oxaloacetate and their growth rate. We used paired linear regression analysis, which determines the inclination angles of the linear growth of the fluorescence ratio, and covariance analysis (ANCOVA), which allows comparing these inclination angles in different ligands and comparing the mean fluorescence ratio values.

A summary of the parameters of the fitted pairwise linear regression equations, coefficients of determination and standard regression errors are shown in Table 1. All fitted models are statistically significant and have good quality: determination coefficients (R^2) are from 0.70 to 0.77. Standard regression errors are from 2.5×10^{-3} to 3.43×10^{-3}.

Fig. 3 shows the slope angles of the regression lines (parameters b_1 of each equation and its 95% confidence interval).

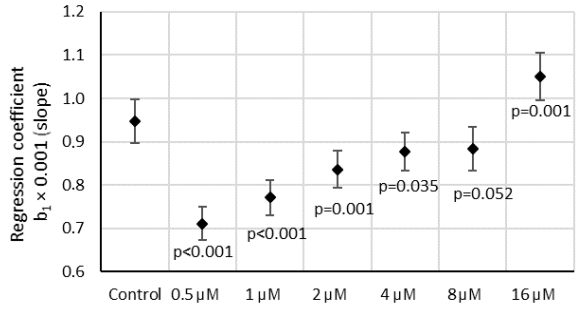

Fig. 3 Angles of regression equations of fluorescence ratio growth when HPA is heated in the temperature range from 20 to 40 °C when oxaloacetate is added at different concentrations: regression coefficients b_1 and their 95% CI

Covariance analysis presents a pooled linear model for controlling and varying ligand concentrations (Table 2).

According to the model, ANCOVA mean values of fluorescence ratio in the middle of the studied temperature range are as follows (95% confidence intervals are given in parentheses):

Control: 0.817 (95% CI: 0.817–0.818),
0.5 µM: 0.753 (95% CI: 0.753–0.753),
1 µM: 0.757 (95% CI: 0.756–0.757),
2 µM: 0.775 (95% CI: 0.775–0.775),
4 µM: 0.778 (95% CI: 0.777–0.778),
8 µM: 0.791 (95% CI: 0.790–0.791),
16 µM: 0.829 (95% CI: 0.829–0.829).

As shown in Figs. 1 and 2, and in Table 2, fluorescence ratios are lower at the probe with oxaloacetate concentration of 0.5–8 µM (all $p < 0.001$), than in the control, the lowest ligand concentration being 0.5 µM. Conversely, higher average fluorescence ratios were detected at a ligand concentration of 16 µM ($p < 0.001$).

As for the comparison of the growth rate of fluorescence ratios when heated to 40 °C, lower values were obtained for a ligand concentration of 0.5–2 µM (all $p < 0.001$) than in the control sample. Close to control but slightly lower for oxaloacetate concentrations 4 and 8 µM ($p = 0.035$ and $p = 0.052$) and higher fluorescence ratio growth rates were noted for a concentration of 16 µM ($p = 0.001$).

In the next step, we studied the effect of oxaloacetate on the conformational stability of GPDH when the enzyme was heated to melting point. To do this, we selected different variants of nonlinear regression models, so that on the one hand there was an acceptable approximation quality, and on the other hand, that regression parameters had a good biochemical interpretation, since the goal of the simulation is to compare the parameters found at different concentrations of small molecules.

We considered a number of possible models: sinusoidal, S-shaped, Hill's equation, cubic parabola. As a result of a detailed analysis of mathematical models, it was decided to use a cubic parabola of the following form:

$$f(t) = d \times (t - b)^3 + c \times t + a, \qquad (1)$$

where $f(t)$ is a dependent variable, fluorescence ratio; t – independent variable, temperature, °C; *a, b, c, d* are parameters of the equation, or regression coefficients.

The choice of this mathematical model for the present study is due to the simplicity and convenient meaningful interpretation of its parameters: b – corresponds to the theoretical inflection point during melting or the average denaturation temperature Tm (°C). Indeed, the second derivative $f(t)$ is as follows:

$$\frac{d^2 f(t)}{dt^2} = 6 \times d \times (t - b). \qquad (2)$$

Equating $6 \times d \times (t - b)$ to zero, we get $t = b$.

Parameter c corresponds to the maximum melting rate. This is proved as follows. The first derivative of the function $f(t)$ is calculated:

$$\frac{df(t)}{dt} = 3 \times d \times (t - b)^2 + c. \qquad (3)$$

At the temperature of the inflection point: $t = b$, the value of the first derivative and, accordingly, the melting rate of the protein is obtained equal to the parameter *c*.

Comparison of different concentrations of oxaloacetate was carried out by the method of confidence intervals: their overlap indicates the statistical indistinguishability of these parameters, and non-overlap indicates the statistical significance of differences in the melting parameter under study.

To build models, a temperature range of 44–56 °C was chosen. The approximation quality for different oxaloacetate concentrations was very different (Table 3, Fig. 4). Thus, for ligand concentrations from 0.5 to 8 mkM, the coefficients of determination were from 0,64 to 0,84, which characterizes the models as fairly accurate.

Table 2 Parameters of the combined ANCOVA model for the dependence of the GPDH fluorescence ratio on the temperature in the range from 20 to 40 °C when oxaloacetate is added at different concentrations.

	b, × 10^{-3}	**SE b, × 10^{-3}**	**p**
Intercept	789.09	0.708	<0.001
temperature	0.95	0.023	<0.001
0.5 µM	–57.58	1.001	<0.001
1 µM	–55.52	1.001	<0.001
2 µM	–39.25	1.001	<0.001
4 µM	–37.82	1.001	<0.001
8 µM	–25.00	1.001	<0.001
16 µM	8.39	1.001	<0.001
Control	reference	–	–
Interaction Effects			
0.5 µM × temperature	–0.24	0.033	<0.001
1 µM × temperature	–0.18	0.033	<0.001
2 µM × temperature	–0.11	0.033	0.001
4 µM × temperature	–0.07	0.033	0.035
8 µM × temperature	–0.06	0.033	0.052
16 µM × temperature	0.10	0.033	0.001
Control × temperature	reference	–	–

Note: b – regression coefficients; SE b – standard errors of regression coefficients; p – significance level.

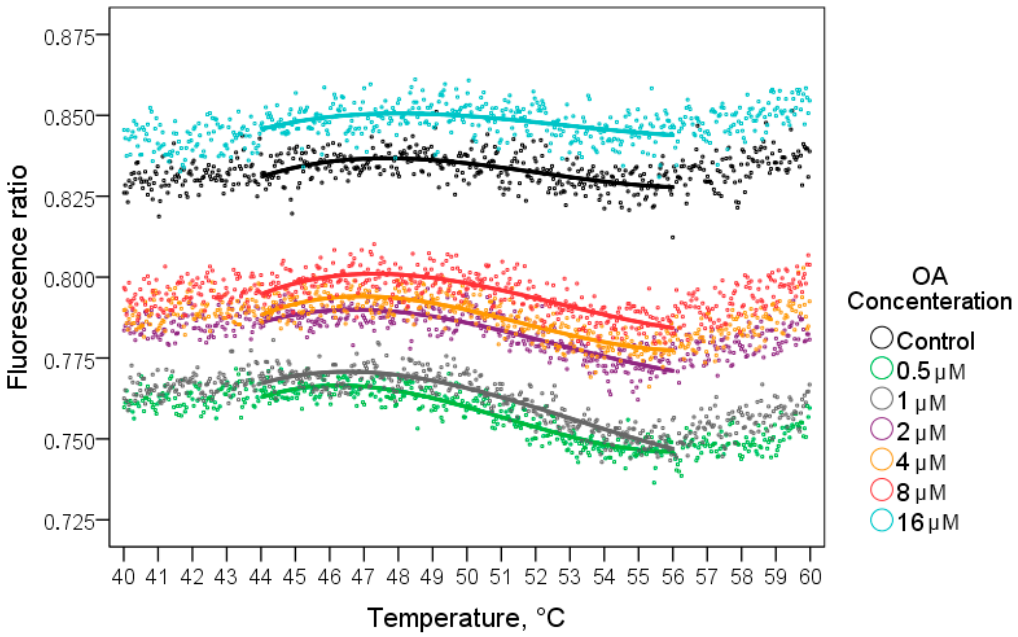

Fig. 4 Ratio of fluorescences during GPDH melting in the temperature range from 44 to 56 °C when oxaloacetate is added at different concentrations: observed values and approximation by cubic parabola.

At the same time, for the reference sample model, the R^2 determination coefficient is 0.33, and for a sample with an oxaloacetate concentration of 16 µM R^2 a total of 0.16. The standard regression errors for all models are in the 0.003–0.005 range.

Table 3 Summary of nonlinear models of dependence of fluorescence ratio at melting of GPDH in temperature range from 44 to 56 °C at addition of oxaloacetate at different concentrations.

	a	b	c, × 10^{-3}	d, × 10^{-6}	R^2	p
Control	0.911±0.007	52.13±0.66	–1.51±0.13	25.15±7.07	0.33	<0.001
0.5 μM	0.917±0.006	51.15±0.19	–3.14±0.11	43.46±5.34	0.84	<0.001
1 μM	0.934±0.007	53.10±0.77	–3.35±0.14	25.76±6.11	0.82	<0.001
2 μM	0.923±0.006	52.59±0.70	–2.72±0.12	26.41±6.71	0.71	<0.001
4 μM	0.923±0.006	51.62±0.30	–2.66±0.12	40.10±6.31	0.70	<0.001
8 μM	0.928±0.007	52.66±0.64	–2.58±0.13	29.95±6.74	0.64	<0.001
16 μM	0.907±0.008	52.83±1.45	–1.13±0.16	16.37±7.95	0.16	<0.001

Note: a –parameter of the equation; b – parameter of the equation, corresponds theoretical inflection point during melting or average denaturation temperature Tm, °C; c – parameter of the equation, corresponds the maximum melting rate of GPDH at inflection point; d – parameter of the equation; R^2 – coefficient of determination; p – significance level.

A graphical representation of the regression parameter b characterizing the temperature of the inflection point at which the melting rate is maximum is shown in Fig. 5. Overlapping confidence intervals of parameter b indicate that inflection points at different intermediate concentrations do not differ.

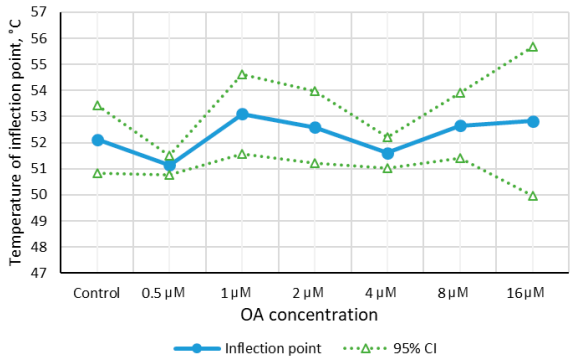

Fig. 5 Inflection points of fluorescence ratios during GPDH melting in the temperature range from 44 to 56 °C with addition of oxaloacetate at different concentrations. The regression coefficients b from the cubic model (solid line) and their 95% CI (dotted lines) are given.

The maximum melting rates according to the fitted mathematical models differ significantly (Fig. 6). Since the fluorescence ratios decrease when the protein melts, the velocities have a negative sign. The fastest melting (the highest absolute value parameters with corresponding to the first derivatives at the inflection point) was noted for GPDH in the presence of oxaloacetate at a concentration of 0.5 μM and 1 μM. A smaller, but also significantly different melting rate is characteristic of ligand concentrations of 2 to 8 μM. Finally, the presence of 16 μM oxaloacetate in the sample did not cause the melting rate to differ from the control sample.

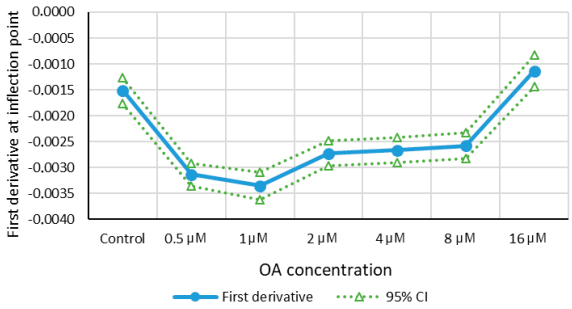

Fig. 6 Maximum melting rates of GPDH in the temperature range from 44 to 56 °C with addition of oxaloacetate at different concentrations. Regression coefficients *c* from cubic model (solid line) and their 95% CI (dotted lines) are given.

4 Conclusions

The experiment demonstrates that the total amplitude of the fluorescence signal in the process of heating the enzyme changed. The effect of biologically active compounds on the fluorescence ratio differs in the area of low concentrations (0.5 and 1 μM) and high concentrations (16 μM). In the physiological temperature range, a linear increase in the fluorescence ratio by an average of $0.95 \pm 0.024 \times 10^{-3}$ for each degree of heating occurs when heated from 20 to 40 °C. Oxaloacetate concentrations of 0.5 μM and 1 μM cause the most significant decreases in fluorescence ratios and its growth rate compared with the control, which mediates the folding of the protein molecule and increases the thermodynamic stability of glycerophosphate dehydrogenase. Oxaloacetate concentrations of 16 μM cause an increase in the fluorescence ratio and an increase in its growth rate, which results in unfolded conformation of the enzyme molecule and a decrease in thermostability.

Documenting and interpreting interactions between metabolites and proteins in a biological context is expected to be important for assessing human health, helping researchers understand the molecular basis of normal and pathological conditions. In particular, regulators of metabolites associated with changes in protein structure may provide new strategies for potential therapeutic interventions.

Disclosures

All authors declare that there is no conflict of interests in this paper.

References

1. E. L. Van Nostrand, S. C. Huelga, and G. W. Yeo, "Experimental and Computational Considerations in the Study of RNA-Binding Protein-RNA Interactions," Advances in Experimental Medicine and Biology 907, 1–28 (2016).
2. E. A. Ryskina, N. A. Kolotyeva, F. N. Gilmiyarova, and N. N. Chernov, "Intermolecular interaction of proteins and small molecules (review)," European Journal of Natural History 3, 8–13 (2016).
3. K. Rooijers, C. M. Markodimitraki, F. J. Rang, S. S. de Vries, A. Chialastri, K. L. de Luca, D. Mooijman, S. S. Dey, and J. Kind, "Simultaneous quantification of protein-DNA contacts and transcriptomes in single cells," Nature Biotechnology 37(7), 766–772 (2019).
4. Q. Xu, R. L. Dunbrack Jr., "ProtCID: a data resource for structural information on protein interactions," Nature Communications 11(1), 711 (2020).
5. Y. Mugabo, S. Zhao, A. Seifried, S. Gezzar, A. Al-Mass, D. Zhang, J. Lamontagne, C. Attane, P. Poursharifi, J. Iglesias, E. Joly, M.-L. Peyot, A. Gohla, S. R. Murthy Madiraju, and M. Prentki, "Identification of a mammalian glycerol-3-phosphate phosphatase: role in metabolism and signaling in pancreatic beta-cells and hepatocytes," Proceedings of the National Academy of Sciences 113(4), 430–439 (2016).
6. E. Possik, S. R. Murthy Madiraju, and M. Prentki, "Glycerol-3-phosphate phosphatase/PGP: Role in intermediary metabolism and target for cardiometabolic diseases," Biochimie 143, 18–28 (2017).
7. P. K. Langston, A. Nambu, J. Jung, M. Shibata, H. I. Aksoylar, J. Lei, P. Xu, M. T. Doan, H. Jiang, M. R. MacArthur, X. Gao, Y. Kong, E. T. Chouchani, J. W. Locasale, N. W. Snyder, and T. Horng, "Glycerol phosphate shuttle enzyme GPD2 regulates macrophage inflammatory responses," Nature Immunology 20(9), 1186–1195 (2019).
8. J. Lu, Z. Xu, H. Duan, H. Ji, Z. Zhen, B. Li, H. Wang, H. Tang, J. Zhou, T. Guo, B. Wu, D. Wang, Y. Liu, Y. Niu, and R. Zhang, "Tumor-associated macrophage interleukin-β promotes glycerol-3-phosphate dehydrogenase activation, glycolysis and tumorigenesis in glioma cells," Cancer Science 111(6), 1979–1990 (2020).
9. C. Zhou, J. Yu, M. Wang, J. Yang, H. Xiong, H. Huang, D. Wu, S. Hu, Y. Wang, X.-Z. Chen, and J. Tang, "Identification of glycerol-3-phosphate dehydrogenase 1 as a tumour suppressor in human breast cancer," Oncotarget 8(60), 101309–101324 (2017).
10. P. Rusu, C. Shao, A. Neuerburg, A. A. Acikgöz, Y. Wu, P. Zou, P. Phapale, T. S. Shankar, K. Döring, S. Dettling, H. Körkel-Qu, G. Bekki, B. Costa, T. Guo, O. Friesen, M. Schlotter, M. Heikenwalder, D. F. Tschaharganeh, B. Bukau, G. Kramer, P. Angel, C. Herold-Mende, B. Radlwimmer, and H.-K. Liu, "GPD1 Specifically Marks Dormant Glioma Stem Cells with a Distinct Metabolic Profile," Cell Stem Cell 25(2), 241–257 (2019).
11. F. Lorenzetti, A. M. Capiglioni, R. A. Marinelli, M. C. Carrillo, and M. de Luján Alvarez, "Hepatic glycerol metabolism is early reprogrammed in rat liver cancer development," Biochimie 170, 88–93 (2020).
12. D. L. Nelson, M. M. Cox, and A. L. Lehninger, Lehninger principles of biochemistry, W. H. Freeman, New York, 2013.
13. F. Campos, T. Sobrino, P. Ramos-Cabrer, and J. Castillo, "Oxaloacetate: A novel neuroprotective for acute ischemic stroke," The International Journal of Biochemistry & Cell Biology 44(2), 262–265 (2012).
14. R. H. Swerdlow, R. Bothwell, L. Hutfles, J. M. Burns, and G. A. Reed, "Tolerability and pharmacokinetics of oxaloacetate 100 mg capsules in Alzheimer's subjects," BBA Clinical 5, 120–123 (2016).
15. H. M. Wilkins, S. Koppel, S. M. Carl, S. Ramanujan, I. Weidling, M. L. Michaelis, E. K. Michaelis, and R. H. Swerdlow, "Oxaloacetate enhances neuronal cell bioenergetic fluxes and infrastructure," Journal of Neurochemistry 137(1), 76–87 (2016).
16. G. R. Grimsley, S. R. Trevino, R. L. Thurlkill, and J. M. Scholtz, "Determining the conformational stability of a protein from urea and thermal unfolding curves," Current Protocols in Protein Science 71(1), 28.4.1–28.4.14 (2013).
17. C. G. Alexander, R. Wanner, C. M. Johnson, D. Breitsprecherc, G. Winterb, S. Duhrc, P. Baaskec, and N. Fergusona, "Novel microscale approaches for easy, rapid determination of protein stability in academic and commercial settings," Biochimica et Biophysica Acta (BBA) – Proteins and Proteomics 1844(12), 2241–2250 (2014).